Helix A Stabilization Precedes Amino-Terminal Lobe Activation upon Calcium Binding to Calmodulin†

Baowei Chen, David F. Lowry, M. Uljana Mayer, and Thomas C. Squier*

Cell Biology and Biochemistry Group, Biological Sciences Division, Pacific Northwest National Laboratory, P.O. Box 999, Richland, Washington 99352

Received April 1, 2008; Revised Manuscript Received June 26, 2008

ABSTRACT: The structural coupling between opposing domains of CaM was investigated using the conformationally sensitive biarsenical probe 4,5-bis(1,3,2-dithioarsolan-2-yl)resorufin (ReAsH), which upon binding to an engineered tetracysteine motif near the end of helix A (Thr-5 to Phe-19) becomes highly fluorescent. Changes in conformation and dynamics are reflective of the native CaM structure, as there is no change in the $^{1}H-^{15}N$ HSQC NMR spectrum in comparison to wild-type CaM. We find evidence of a conformational intermediate associated with CaM activation, where calcium occupancy of sites in the amino-terminal and carboxyl-terminal lobes of CaM differentially affect the fluorescence intensity of bound ReAsH. Insight into the structure of the conformational intermediate is possible from a consideration of calcium-dependent changes in rates of ReAsH binding and helix A mobility, which respectively distinguish secondary structural changes associated with helix A stabilization from the tertiary structural reorganization of the amino-terminal lobe of CaM necessary for high-affinity binding to target proteins. Helix A stabilization is associated with calcium occupancy of sites in the carboxyl-terminal lobe ($K_d = 0.36 \pm 0.04$ μM), which results in a reduction in the rate of ReAsH binding from 4900 M^{-1} s^{-1} to 370 M^{-1} s^{-1}. In comparison, tertiary structural changes involving helix A and other structural elements in the amino-terminal lobe require calcium occupancy of amino-terminal sites ($K_d = 18 \pm 3$ μM). Observed secondary and tertiary structural changes involving helix A in response to the sequential calcium occupancy of carboxyl- and amino-terminal lobe calcium binding sites suggest an important involvement of helix A in mediating the structural coupling between the opposing domains of CaM. These results are discussed in terms of a model in which carboxyl-terminal lobe calcium activation induces secondary structural changes within the interdomain linker that release helix A, thereby facilitating the formation of calcium binding sites in the amino-terminal lobe and linked tertiary structural rearrangements to form a high-affinity binding cleft that can associate with target proteins.

Calmodulin (CaM)[1] is a central regulatory protein, which through reversible and high-affinity association with over 50 different target proteins acts to modulate their function in response to alterations in cytosolic calcium levels (*1*−*3*). High-affinity binding requires the calcium-dependent stabilization of binding clefts in the amino- and carboxyl-terminal lobes of CaM (*4*). The calcium affinities of sites in each domain are, in general, enhanced by target protein association to the extent that they facilitate the correct positioning of calcium binding ligands (*5*−*9*). Conformational plasticity within each of the binding clefts formed by the opposing amino- and carboxyl-terminal lobes of CaM, as well as the calcium-dependent formation of a metastable helix connecting the opposing lobes, contributes to the ability to associate with diverse CaM-binding sequences that bear little sequence homology to one another and have variable spacing between the binding sites (*10*−*14*). Large variations in both orientation and spatial separation occur between the opposing domains of calcium-activated CaM bound to different CaM-binding sequences from target proteins, as evidenced from the 16 available high-resolution crystal structures (*15*). These results emphasize the essential role of the conformational linker connecting the opposing domains of CaM in facilitating high-affinity binding. Further, despite the nearly identical structures of the amino- and carboxyl-terminal lobes of CaM, the opposing domains of CaM bind to target proteins with considerable specificity to form a single high-affinity complex capable of target protein regulation. Contributing to the specificity of CaM binding are large differences in the calcium affinities of the opposing domains. The carboxyl-terminal lobe binds calcium with an affinity that is approximately 1 order of magnitude higher than that of the amino-terminal lobe, promoting its preferential association with target proteins prior to the structural collapse and

† This work was supported by the Genomics:GTL program (45701) within the Office of Biological and Environmental Research at the U.S. Department of Energy. Pacific Northwest National Laboratory is operated for the Department of Energy by Battelle Memorial Institute under Contract DE-AC05-76RLO 1830.

* Correspondence should be addressed to this author. E-mail: thomas.squier@pnl.gov. Tel: (509) 376-2218. Fax: (509) 372-1632.

[1] Abbreviations: β-ME, β-mercaptoethanol; CaM, calmodulin; EDT, 1,2-ethanedithiol; EDTA, ethylenediaminetetraacetic acid; EGTA, ethylene glycol bis(β-aminoethyl ether)-*N*,*N*,*N*′,*N*′-tetraacetic acid; HEPES, *N*-(2-hydroxyethyl)piperazine-*N*′-2-ethanesulfonic acid; HSQC, heteronuclear single-quantum coherence; NOE, nuclear Overhauser effect; ReAsH-EDT_2, 4,5-bis(1,3,2-dithioarsolan-2-yl)resorufin; TCEP, tris(carboxyethyl)phosphine.

10.1021/bi800566u CCC: $40.75
Published on Web 08/09/2008

binding of the amino-terminal lobe (*16, 17*). This greater calcium affinity of the carboxyl-terminal lobe of CaM is especially important in the case of some ion channels, including the ryanodine receptor calcium release channel, where the carboxyl-terminal lobe binds calcium under resting conditions (*18*). By tethering CaM to the channel, enhanced rates of channel inhibition are possible upon the calcium activation of the amino-terminal lobe through a reduction of diffusional barriers (*18*−*21*).

Understanding the origins of differences in the calcium affinities of the structurally homologous amino- and carboxyl-terminal lobes of CaM, and how partial calcium occupancy affects their coupling to enhance the specificity of target protein binding, is central to our understanding of CaM action. Prior measurements have demonstrated that calcium binding modulates the structural coupling between the opposing domains of CaM, acting to stabilize the helical structure of the interfacial residues between Met-76 and Ser-81 (*13, 14, 22, 23*). Indeed, occupancy of carboxyl-terminal calcium binding sites induces conformational changes in the amino-terminal domain, which is apparent from both changes in fluorescence signals of reporter moieties and from increased rates of proteolysis at selected sites in the amino-terminal lobe (*14, 24, 25*). Further, the structural coupling between the opposing domains of CaM is stabilized at physiological ionic strengths, which acts to diminish the calcium affinity of sites in the amino-terminal lobe (*13, 26*). These latter results suggest an important role for calcium-dependent structural changes involving interfacial amino acids in the structural coupling between the opposing amino- and carboxyl-terminal lobes of CaM that acts to modulate calcium binding. Consistent with this suggestion, the isolated amino-terminal lobe of CaM has a substantially enhanced calcium affinity in comparison to that observed in the intact protein (*27*). A systematic investigation by Shea and co-workers provided further insight into the mechanism of interdomain structural coupling, demonstrating that the presence of basic residues in the linker region connecting the opposing lobes of CaM diminish the calcium binding affinity of the amino-terminal lobe (*28, 29*). There are corresponding alterations in the thermodynamic stability of the amino-terminal domain, suggesting a structural role for these side chains that are proposed to be "latched" to amino acids in helix A (i.e., Thr-5 to Phe-19) to increase the energetic barrier associated with calcium activation (*28*). Consistent with this suggestion, high-resolution structures of apo- and calcium-activated CaM indicate that the disruption of contact interactions between helix A and other amino-terminal residues (e.g., Asp-2) with sites in the central linker (e.g., Lys-77) are necessary for calcium binding at amino-terminal lobe sites (Figure 1). This conformational switching has been previously measured using the biarsenical probe FlAsH bound to helix A, which resolves the calcium-dependent stabilization of the linker connecting the amino- and carboxyl-terminal lobes from the immobilization of helix A associated with the formation of the high-affinity calcium binding cleft necessary for target protein binding (*30, 31*).

To further understand the role of helix A in modulating the coupling between the opposing domains of CaM in response to calcium activation, we have used the biarsenical probe 4,5-bis(1,3,2-dithioarsolan-2-yl)resorufin (ReAsH) to measure changes in helix A dynamics upon the partial

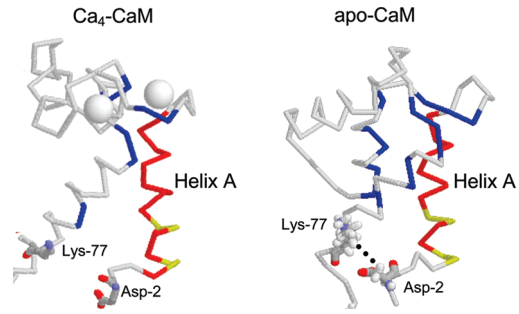

FIGURE 1: Loss of helix A long-range helical contact interactions upon calcium activation of CaM. Depiction of backbone folds for N-terminal lobe of calcium-activated CaM (1exr.pdb) and apo-CaM (1cfd.pdb), highlighting contact interactions between helix A (red) with engineered cysteines (yellow) and proximal residues (i.e., <5 Å) within the tertiary structures (blue). Specific side chains previously implicated in mediating interdomain structural interactions include Asp-2 and Lys-77 in the N-terminal lobe (*28*).

occupancy of calcium binding sites in CaM. In comparison to prior measurements using FlAsH, these new measurements take advantage of the enhanced environmental sensitivity, smaller size, and presence of a fully ionized moiety in ReAsH ($pK_a = 5.8$) (*32*), facilitating the measurement and interpretation of calcium-dependent structural changes. These measurements use a CaM mutant with an engineered binding motif within helix A, that remains fully functional (*30*). ReAsH is a conformationally sensitive probe whose rate of binding is dependent on protein secondary structure (*30, 33*−*36*), providing a new tool that permits the detection of structural changes associated with helix distortions or fraying. Complementary fluorescence measurements of ReAsH bound to helix A permit the measurement of calcium binding to amino-terminal lobe sites that are associated with helix A immobilization and the formation of clefts for target protein binding. Together, these binding and fluorescence measurements resolve a conformational intermediate associated with the calcium activation of CaM. Calcium occupancy of sites in the carboxyl-terminal lobe of CaM results in the stabilization of helix A structure through the disruption of distorting interactions. Tertiary structural changes are thereby facilitated that couple calcium binding at the amino-terminal lobe to the tertiary structural coupling between helix A and other structural elements in the amino-terminal lobe, which together form the high-affinity binding cleft necessary for target protein binding.

EXPERIMENTAL PROCEDURES

Materials. *N*-(2-Hydroxyethyl)piperazine-*N*′-2-ethanesulfonic acid (HEPES) and tris(carboxyethyl)phosphine (TCEP) were obtained from Sigma (St. Louis, MO). 2-Mercaptoethanol (β-ME) was obtained from Aldrich (Milwaukee, WI). ^{13}C (98%) and ^{15}N (98%) Bioexpress cell growth media (10× concentrate) was from Cambridge Isotope Laboratories, Inc., (Andover, MA). 4,5-Bis(1,3,2-dithiarsolan-2-yl)resorufin (ReAsH), which contains ethanedithiol (EDT), was synthesized using published procedures (*34*). A CaM mutant containing an engineered tetracysteine binding motif involving the introduction of cysteines at positions E6, E7, A10, and E11 on helix A (Thr-5 to Phe-19) was purified following expression in *Escherichia coli*, as previously described (*30*). For NMR measurements, the *E. coli* was grown in a medium

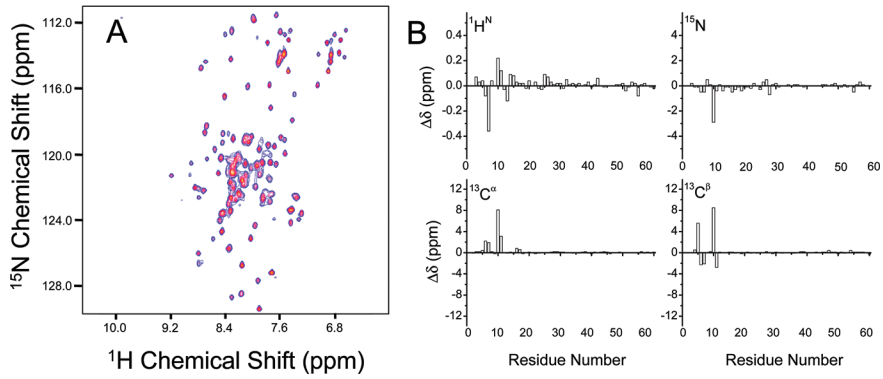

FIGURE 2: Preservation of backbone fold upon mutation of helix A. $^{1}H-^{15}N$ HSQC NMR spectrum of apo-CaM with cysteine tagging sequence engineered at positions 6, 7, 10, and 11 in the primary sequence (A) and measured differences between peak positions for indicated resonances in amino-terminal domains between engineered and wild-type CaM (B), using previously reported assignments (*39*). Contour lines are shown for spectral intensities, where a fire ramp code from blue to red indicates increasing intensities.

uniformly enriched with ^{13}C and ^{15}N, essentially as previously described (*37, 38*). All other chemicals were of the purest grade commercially available.

Spectroscopic Measurements. 2D-HSQC, 3D-CBCA-(CO)NNH, and 3D-HNCACB NMR spectra were acquired at 25 °C using 600 and/or 800 MHz Varian Inova spectrometers equipped with triple-resonance pulse field gradient probes, essentially as we previously described (*38*). Backbone assignments were initially made by comparison to WT CaM assignments (*39*) and then confirmed by a routine backbone walk using the spectra from the two 3D experiments. Fluorescence emission spectra of ReAsH-labeled CaM were measured using a Fluoro Max-2 fluorometer (SPEX Inc., Edison, NJ) using a temperature-jacketed sample cell at 25 °C with excitation and emission slits of 5 nm. Steady-state fluorescence anisotropies (A) were calculated from the ratio of the fluorescence intensity (I) with the polarizers in vertical (v) or horizontal (h) position

$$A = \frac{I_{vv} - gI_{vh}}{I_{vv} + 2gI_{vh}} \quad (1)$$

where $g = I_{hv}/I_{hh}$. Excitation and emission wavelengths were 593 and 608 nm, respectively. In all cases, protein concentrations were measured using a micro-BCA assay reagent kit (Pierce, Rockford, IL), using desalted CaM as a protein standard ($\epsilon_{277nm} = 3029\ M^{-1}\ cm^{-1}$) (*40, 41*). Prior to addition of 1.0 μM ReAsH, the CaM mutant containing the tetracysteine motif in helix A was incubated for 1 h at room temperature in 1 mM β-ME, and 1 mM TCEP to reduce any disulfide bonds. All experiments involved CaM (1.0 μM) in 50 mM HEPES (pH 7.5), 140 mM KCl, 1.0 mM EGTA, and sufficient calcium to generate the indicated free calcium concentration, as previously described (*23*).

Calcium Binding Affinities. Data were analyzed through a nonlinear least-squares fit to changes in fluorescence intensities (Y) to the Hill equation:

$$Y = \frac{[Ca^{2+}]^{n}_{free}}{K^{n} + [Ca^{2+}]^{n}_{free}} \times \text{span} + Y_0 \quad (2)$$

where n is the Hill coefficient and K is the macroscopic dissociation constant, which represents the sum of the microscopic equilibrium binding constants (i.e., $k_1 + k_2$) for homotropic cooperativity (*42*), span is the range of the measurement, and Y_0 is the initial fluorescence observed at low calcium levels whose concentrations preclude binding to CaM.

RESULTS

Retention of CaM Tertiary Structure Following Introduction of Engineered Binding Sequence. To assess the possible influence of an engineered tagging sequence (i.e., E6C, E7C, A10C, and E11C) in helix A (Thr-5 to Phe-19) on the protein fold, we measured the change in backbone chemical shifts between wild-type and mutant CaM. Resonances in the HSQC spectrum are well resolved, and the line widths and chemical shifts of the resonances are virtually identical to that observed in prior measurements using wild-type CaM (*39*) (Figure 2). Indeed, small shifts in resonance positions are limited to the mutated sites, and even at the millimolar protein concentrations used in these NMR measurements there is no evidence of protein associations. Furthermore, changes in backbone ^{13}C-α shifts near the mutation sites are in the positive direction and are not indicative of helix disruption. Thus, NMR spectroscopic measurements demonstrate a retention of the native CaM structure upon insertion of mutated sites on helix A, consistent with the exterior location of these engineered binding sites and prior measurements demonstrating a full retention of binding affinity and functional activation against target proteins (*30, 43*). These results indicate that measurements using the engineered CaM mutant with a tetracysteine motif in helix A will faithfully reflect the native structure of CaM.

Helix A Stabilization upon Calcium Occupancy of Carboxyl-Terminal Sites. ReAsH and other biarsenical probes selectively bind to disordered sequences (*34*), providing a unique tool for measuring variations in secondary structural changes involving protein backbone elements such as helix A in CaM through a consideration of binding kinetics (*30, 31, 34−36*). Measurements of ReAsH binding to helix A in CaM are facilitated by large changes in the fluorescence intensity of the bound complex, as prior to association with helix A ReAsH exhibits minimal fluorescence due to capping with ethanedithiol (EDT) (*34*). We find that upon addition of ReAsH to apo-CaM at low calcium levels (i.e., 10 nM free calcium) there is a rapid increase in fluorescence intensity, where maximal binding occurs in about 10 min (Figure 3A). Rates of ReAsH binding to helix A are substantially diminished upon the calcium-dependent activa-

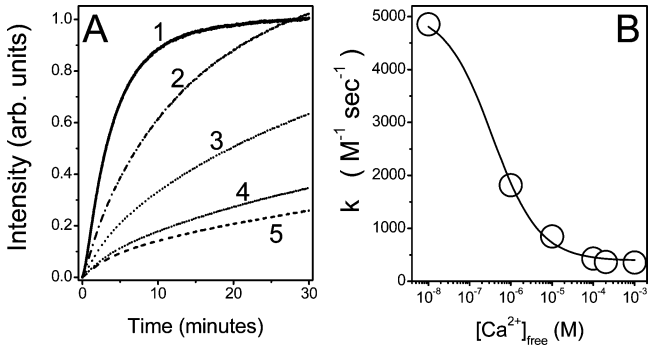

FIGURE 3: Calcium binding to C-terminal domain stabilizes helix A. Fluorescence intensity increases upon binding of biarsenical probe ReAsH to helix A (A) and calculated initial rate constants (B), where selected binding curves are illustrated corresponding to free calcium concentrations ranging from 0.01 μM (curve 1), 1.0 μM (curve 2), 10 μM (curve 3), 100 μM (curve 4), and 1.0 mM (curve 5). Rate constants were calculated from the data in panel A, taking into account that the initial concentrations of reactants and products are identical, such that the rate law simplifies to $1/[\text{ReAsH}]_t - 1/[\text{ReAsH}]_{t=0} = kt$, where $[\text{ReAsH}]_{t=0}$ and [ReAsH] are the initial and remaining concentrations of unbound ReAsH (*30*). The line in panel B corresponds to nonlinear least-squares fit to the calcium-dependent decrease in the rates of ReAsH binding using the Hill equation, where the macroscopic equilibrium constant (K_d) is 0.36 $\pm$ 0.04 μM free calcium and $n = 0.8 \pm 0.1$. Excitation was at 593 nm, and fluorescence emission was measured at 608 nm at 25 °C. Experimental conditions involved the addition of 1.0 μM ReAsH-EDT$_2$ to 1.0 μM CaM in 50 mM HEPES (pH 7.5) 140 mM KCl, 1.0 mM EGTA, 1 mM β-ME, 1 mM TCEP, and sufficient calcium to yield the indicated free calcium concentration, as previously described (*23*).

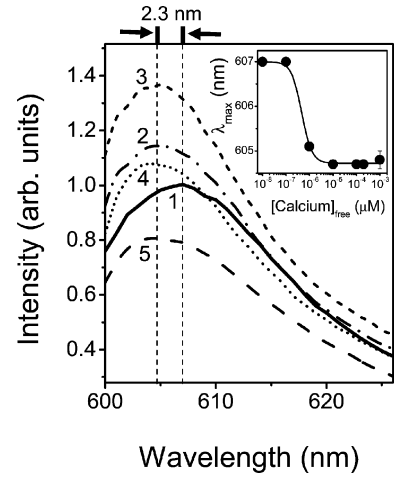

FIGURE 4: Calcium binding to the C-terminal domain induces environmental shifts around helix A. Fluorescence emission spectra and shifts in fluorescence emission maximum (inset) for ReAsH-labeled CaM, where free calcium concentrations range from 0.01 μM (curve 1), 1.0 μM (curve 2), 10 μM (curve 3), 100 μM (curve 4), and 1.0 mM (curve 5). The line in the inset represents a nonlinear least-squares fit to the Hill equation, where $K_d = 0.46 \pm 0.04$ μM and $n = 2$. Excitation was at 593 nm. Experimental conditions involve 1.0 μM ReAsH-labeled CaM in 50 mM HEPES (pH 7.5) 140 mM KCl, 1.0 mM EGTA, 1 mM β-ME, 1 mM TCEP, and sufficient calcium to yield the indicated free calcium concentration, as in Figure 3.

tion of CaM, where the rate of binding is decreased from 4900 M^{-1} s^{-1} in apo-CaM to 370 M^{-1} s^{-1} following calcium activation. Rates of ReAsH binding approach a minimal value near a free calcium concentration of 10 μM. Decreases in the rates of ReAsH binding to helix A have a calcium dependence that mirrors that associated with the occupancy of calcium sites in the carboxyl-terminal lobe of CaM (*23, 44*−*46*), with a macroscopic dissociation constant for calcium binding of 0.36 $\pm$ 0.04 μM (Figure 3B). As the crystal structures and prior measurements of solvent accessibilities have demonstrated that there is no calcium-dependent change in the solvent exposures of the engineered tetracysteine binding sites (*30*), these results indicate that calcium binding to sites in the carboxyl-terminal lobe of CaM acts to induce the formation of a more regular secondary structure in helix A.

Detection of Conformational Intermediates Associated with Calcium Activation. Additional resolution of calcium-dependent structural changes to helix A involves measurements of the fluorescence emission spectra of bound ReAsH, which provide a means to assess changes in the immediate environment of the labeling site to assess the nature of the structural change. The fluorescence emission spectrum of ReAsH bound to apo-CaM has an emission maximum near 607 nm (Figure 4). Upon titration of free calcium levels, we observe a biphasic dependence of the fluorescence emission spectrum. There is a 36% increase in fluorescence intensity and a corresponding 2.3 nm blue shift in the fluorescence emission spectrum upon increasing the free calcium concentration to 10 μM, where the macroscopic equilibrium constant for the measured calcium-dependent structural change is 0.46 $\pm$ 0.04 μM. The significant blue shift in the emission spectrum of ReAsH-bound to helix A upon occupancy of carboxyl-terminal calcium binding sites is indicative of a more polar environment, as greater solvent polarity results in a large increase in the quantum yield and a blue shift of the parent dye resorufin (*32*). This result is consistent with the formation of a more regular helical structure that, for example, brings Asp-2 or Glu-14 into closer proximity of the bound probe located at positions 6, 7, 10, and 11 on helix A (i.e., Thr-5 to Phe-19). This interpretation is consistent with decreases in the rates of ReAsH binding that suggest a disruption of long-range structural interactions involving helix A over this calcium concentration range (Figure 3). In comparison to this intermediate state, increases in free calcium levels from 10 μM to 1 mM, which are associated with the titration of calcium binding sites in the amino-terminal domain, result in a 40% decrease in fluorescence intensity with no change in fluorescence emission maximum. These latter results suggest that distinct conformational rearrangements involving helix A occur in response to the occupancy of calcium binding sites in the carboxyl- and amino-terminal lobes. The large decrease in fluorescence intensity coupled with the absence of any spectral shifts upon calcium binding to the amino-terminal sites suggests that a rigid body movement of a stabilized helix A, and an associated increase in solvent exposure of bound ReAsH, is associated with the formation of the binding cleft for target protein association.

Calcium Binding to Sites in the Amino-Terminal Lobe Result in Helix A Immobilization. The calcium-dependent formation of the high-affinity binding cleft involves tertiary structural interactions between helix A and other elements in the amino-terminal lobe, which can be measured through changes in the fluorescence anisotropy of ReAsH. This is possible since ReAsH faithfully reports on helix A dynamics due to the tetracoordinate linkage that prevents independent probe motion. These measurements permit us to assess the

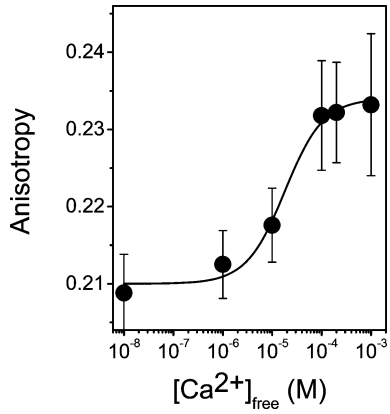

FIGURE 5: Occupancy of N-terminal calcium binding sites induces coupling between helix A and N-terminal lobe structural elements to form a high-affinity binding cleft. Calcium-dependent changes in fluorescence anisotropy of ReAsH-labeled CaM, using experimental conditions as described in the legend to Figure 4. The line represents a nonlinear least-squares fit to the Hill equation, where $K_d = 18 \pm 3$ μM and $n = 1.1 \pm 0.2$. Experimental conditions are as described in the legend to Figure 4.

possible relationship between secondary structural changes associated with helix A from tertiary changes involving the coordinated formation of a high-affinity binding cleft. Upon calcium activation there is a small but highly reproducible increase in the fluorescence anisotropy of ReAsH-labeled CaM, which increases from 0.208 to 0.234 (Figure 5). These measurements are consistent with prior results that indicate only small changes in secondary structure upon calcium activation, which result in the immobilization of helix A and the structural coupling between the opposing amino- and carboxyl-terminal lobes of CaM (*30, 47*−*50*). From a consideration of calcium-dependent changes in fluorescence anisotropy, it is apparent that there are minimal changes in helix A mobility prior to increasing calcium concentrations above 10 μM free calcium. These results suggest an insensitivity of helix A mobility to the occupancy of calcium sites in the carboxyl-terminal lobe of CaM. Rather, increases in helix A immobilization occur upon titration of calcium binding sites in the amino-terminal lobe ($K_d = 18 \pm 3$ μM). Observed secondary and tertiary structural changes involving helix A in response to the sequential calcium occupancy of carboxyl- and amino-terminal lobe calcium binding sites provide important mechanistic information regarding an important involvement of helix A in mediating the structural coupling between the opposing domains of CaM.

DISCUSSION

We have identified distinct and nonoverlapping structural transitions involving helix A (Thr-5 to Phe-19) that are associated with the sequential occupancy of carboxyl- and amino-terminal lobe calcium binding sites, which indicates the presence of a conformationally distinct intermediate that provides new insights regarding the mechanisms of calcium activation in CaM. These measurements required the application of newly developed probes that detect conformational transitions in helical structures (*34*), which are known to vary considerably in available high-resolution protein structures in response to their environment, involving, for example, differences in van der Waals contact interactions with other structural elements in the protein that distort helical structures (*51*). Specifically, the conformationally and environmentally sensitive biarsenical fluorescent probe ReAsH permitted the detection of structurally distinct forms of helix A in response to calcium binding to the carboxyl- and amino-terminal sites in CaM. Upon calcium association with sites in the carboxyl-terminal lobe ($K_d = 0.4$ μM free calcium), we observe the stabilization of the secondary structure of helix A (Figures 3 and 4). In comparison, we detect a structural reorganization involving helix A movements upon calcium binding to the amino-terminal lobe ($K_d = 18$ μM free calcium), which is associated with the formation of the binding cleft for target protein association (Figure 5). The detection of sequential conformational transitions involving helix A upon the calcium-dependent activation of CaM is consistent with a wide variety of prior measurements, which all indicate a structural linkage between the opposing amino- and carboxyl-terminal lobes of CaM through a conformational intermediate that is modulated by calcium binding (*12*−*14, 24, 25, 29*−*31, 52*−*54*).

Our current results suggest that calcium binding to sites in the carboxyl-terminal lobe disrupts destabilizing interactions involving helix A, thereby resulting in a 92% decrease in the rate of ReAsH binding (Figure 3). Corresponding red shifts in the fluorescence emission spectrum are consistent with formation of a more regular helix, which would be expected to result in the juxtaposition of charged amino acids positioned approximately one turn within an α-helix (e.g., Asp-2 or Glu-14) relative to the engineered ReAsH binding site (i.e., E6C, E7C, A10C, and E11C). The observed stabilization of helix A can be explained as part of a conformational "switch" that acts to enhance calcium binding to amino-terminal lobe sites. Indeed, prior measurements have identified a structural interaction between helix A (and proximal amino acids in the primary sequence) and basic residues in the central linker (i.e., RKMK[77]) that act as a "latch" to enhance the stability and reduce the calcium affinity of the amino-terminal lobe (*28, 29, 44*). As calcium activation enhances the helical content of the central linker through the formation of a salt bridge between Tyr-138 and Glu-82 to modify the orientation of the opposing domains of CaM (*12, 13, 22*), our current results suggest that the release of helix A acts to enhance calcium binding to amino-terminal lobe sites. Changes in helix A structure involve calcium-dependent alterations in interdomain linkages through side chains in the central linker (Arg-76 to Ser-81) and those in both the carboxyl- and amino-terminal domains (*12, 28*). Specifically, calcium activation involves the repositioning of C-terminal helices to form a hydrogen bond involving Tyr-138 and Glu-82. This hydrogen bond enhances helical content, which acts to disrupt the latch mechanism involving interactions between basic side chains in the central linker (e.g., Lys-77) and residues near the amino terminus (e.g., Asp-2) to release helix A (Figure 6). Subsequent calcium binding to sites in the amino-terminal lobe functions to reposition helical structural elements to form the high-affinity binding cleft necessary for target protein activation.

The structural linkage between helix A and the central linker acts to constrain the dynamics of the amino-terminal domain of CaM, thereby increasing the activation barrier associated with conformational rearrangements needed to position calcium binding side chains, thereby reducing the calcium affinity from that of the isolated domain (*27*−*29*). Of the basic residues in the central linker, residue Lys-77 is especially noteworthy as this side chain interacts with Asp-2 in the apo form of CaM. This salt bridge is disrupted upon calcium activation, suggesting that it may be a key structural interaction whose formation modulates interdomain coupling and calcium binding affinity

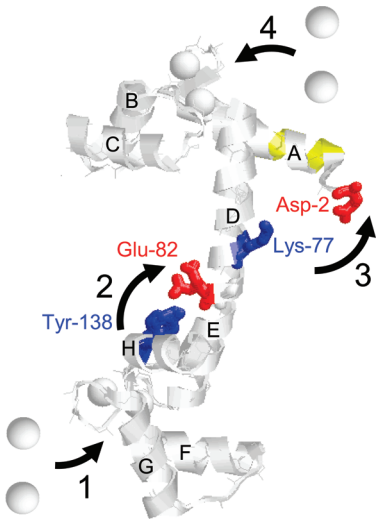

FIGURE 6: Model depicting proposed mechanism of sequential calcium binding to opposing CaM domains. Initial occupancy of C-terminal lobe calcium binding sites (step 1) promotes formation of a salt bridge between Tyr-138 and Glu-82 (step 2) (*12, 66*). The resulting helical stabilization of the interdomain linker and side chain reorientations act to disrupt interactions between helix A and basic side chains in helix D that include Lys-77 and Asp-2 (step 3) (*12, 13, 22*), which has previously been shown to restrict N-terminal lobe dynamics and reduce calcium binding affinity (*28*). Following helix A stabilization, the formation of N-terminal lobe calcium binding sites is facilitated to form a high-affinity binding cleft associated with target protein binding (step 4) (*4*). Letters correspond to individual helical elements. Positions of introduced cysteines are in yellow. Structure corresponds to that of calcium-activated CaM (1exr.pdb) and is represented using the program RASMOL (*67*).

(*28*). Other specific binding interactions between side chains near the amino terminus of apo-CaM (i.e., residues Ala-1, Asp-2, Leu-4, Gln-8, and Phe-12) and those in the central linker (Met-76, Lys-77, and Asp-80) are apparent in the high-resolution structures (i.e., 1cfd.pdb) (*55*), and may also contribute to conformational switching as all but three side chain interactions are lost upon calcium activation (1exr.pdb) (*56*). Following occupancy of calcium binding sites in the carboxyl-terminal lobe, there are concerted structural changes in amino-terminal lobe. The structural coupling between the opposing domains of CaM acts to ensure a large difference in binding affinity between carboxyl- and amino-terminal domain calcium sites, which is likely to promote the ordered binding of the opposing domains of CaM to target proteins. In this respect, the oxidation of critical methionines in the carboxyl-terminal domain of CaM during biological aging and following macrophage activation acts to uncouple the opposing domains of CaM, resulting in the nonproductive binding between CaM and some target proteins to diminish to activities (*31, 37, 57*−*64*). Oxidation of CaM results in the preferential reduction in calcium binding affinity to the C-terminal lobe (*65*). These latter results emphasize a critical role for the sequential activation of the opposing domains of CaM through large differences in their calcium affinities and the role of coupled structural linkages to enforce ordered binding mechanisms to target proteins.

REFERENCES

1. Carafoli, E. (1991) The calcium pumping ATPase of the plasma membrane. *Annu. Rev. Physiol. 53*, 531–547.
2. Chin, D., and Means, A. R. (2000) Calmodulin: a prototypical calcium sensor. *Trends Cell Biol. 10*, 322–328.
3. Crivici, A., and Ikura, M. (1995) Molecular and structural basis of target recognition by calmodulin. *Annu. Rev. Biophys. Biomol. Struct. 24*, 85–116.
4. Vigil, D., Gallagher, S. C., Trewhella, J., and Garcia, A. E. (2001) Functional dynamics of the hydrophobic cleft in the N-domain of calmodulin. *Biophys. J. 80*, 2082–2092.
5. Findlay, W. A., Martin, S. R., Beckingham, K., and Bayley, P. M. (1995) Recovery of native structure by calcium binding site mutants of calmodulin upon binding of sk-MLCK target peptides. *Biochemistry 34*, 2087–2094.
6. Peersen, O. B., Madsen, T. S., and Falke, J. J. (1997) Intermolecular tuning of calmodulin by target peptides and proteins: differential effects on Ca^{2+} binding and implications for kinase activation. *Protein Sci. 6*, 794–807.
7. Tang, W., Halling, D. B., Black, D. J., Pate, P., Zhang, J. Z., Pedersen, S., Altschuld, R. A., and Hamilton, S. L. (2003) Apocalmodulin and Ca^{2+} calmodulin-binding sites on the CaV1.2 channel. *Biophys. J. 85*, 1538–1547.
8. Xiong, L. W., Newman, R. A., Rodney, G. G., Thomas, O., Zhang, J. Z., Persechini, A., Shea, M. A., and Hamilton, S. L. (2002) Lobe-dependent regulation of ryanodine receptor type 1 by calmodulin. *J. Biol. Chem. 277*, 40862–40870.
9. Jurado, L. A., Chockalingam, P. S., and Jarrett, H. W. (1999) Apocalmodulin. *Physiol. Rev. 79*, 661–682.
10. Wriggers, W., Mehler, E., Pitici, F., Weinstein, H., and Schulten, K. (1998) Structure and dynamics of calmodulin in solution. *Biophys. J. 74*, 1622–1639.
11. Chang, S. L., Szabo, A., and Tjandra, N. (2003) Temperature dependence of domain motions of calmodulin probed by NMR relaxation at multiple fields. *J. Am. Chem. Soc. 125*, 11379–11384.
12. Sun, H., Yin, D., Coffeen, L. A., Shea, M. A., and Squier, T. C. (2001) Mutation of Tyr138 disrupts the structural coupling between the opposing domains in vertebrate calmodulin. *Biochemistry 40*, 9605–9617.
13. Sun, H., Yin, D., and Squier, T. C. (1999) Calcium-dependent structural coupling between opposing globular domains of calmodulin involves the central helix. *Biochemistry 38*, 12266–12279.
14. Yao, Y., Schoneich, C., and Squier, T. C. (1994) Resolution of structural changes associated with calcium activation of calmodulin using frequency domain fluorescence spectroscopy. *Biochemistry 33*, 7797–7810.
15. Boschek, C. B., Sun, H., Bigelow, D. J., and Squier, T. C. (2008) Different conformational switches underlie the calmodulin-dependent modulation of calcium pumps and channels. *Biochemistry 47*, 1640–1651.
16. Persechini, A., McMillan, K., and Leakey, P. (1994) Activation of myosin light chain kinase and nitric oxide synthase activities by calmodulin fragments. *J. Biol. Chem. 269*, 16148–16154.
17. Sun, H., and Squier, T. C. (2000) Ordered and cooperative binding of opposing globular domains of calmodulin to the plasma membrane Ca-ATPase. *J. Biol. Chem. 275*, 1731–1738.
18. Boschek, C. B., Jones, T. E., Squier, T. C., and Bigelow, D. J. (2007) Calcium occupancy of N-terminal sites within calmodulin induces inhibition of the ryanodine receptor calcium release channel. *Biochemistry 46*, 10621–10628.
19. Maximciuc, A. A., Putkey, J. A., Shamoo, Y., and Mackenzie, K. R. (2006) Complex of calmodulin with a ryanodine receptor target reveals a novel, flexible binding mode. *Structure 14*, 1547–1556.
20. Zhang, H., Zhang, J. Z., Danila, C. I., and Hamilton, S. L. (2003) A noncontiguous, intersubunit binding site for calmodulin on the skeletal muscle Ca^{2+} release channel. *J. Biol. Chem. 278*, 8348–8355.
21. Rodney, G. G., Moore, C. P., Williams, B. Y., Zhang, J. Z., Krol, J., Pedersen, S. E., and Hamilton, S. L. (2001) Calcium binding to calmodulin leads to an N-terminal shift in its binding site on the ryanodine receptor. *J. Biol. Chem. 276*, 2069–2074.
22. Qin, Z., and Squier, T. C. (2001) Calcium-dependent stabilization of the central sequence between Met(76) and Ser(81) in vertebrate calmodulin. *Biophys. J. 81*, 2908–2918.
23. Boschek, C. B., Squier, T. C., and Bigelow, D. J. (2007) Disruption of interdomain interactions via partial calcium occupancy of calmodulin. *Biochemistry 46*, 4580–4588.
24. Pedigo, S., and Shea, M. A. (1995) Quantitative endoproteinase GluC footprinting of cooperative Ca^{2+} binding to calmodulin: proteolytic susceptibility of E31 and E87 indicates interdomain interactions. *Biochemistry 34*, 1179–1196.
25. Shea, M. A., Verhoeven, A. S., and Pedigo, S. (1996) Calcium-induced interactions of calmodulin domains revealed by quantitative thrombin footprinting of Arg37 and Arg106. *Biochemistry 35*, 2943–2957.
26. Pedigo, S., and Shea, M. A. (1995) Discontinuous equilibrium titrations of cooperative calcium binding to calmodulin monitored

by 1-D ^{1}H-nuclear magnetic resonance spectroscopy. *Biochemistry 34*, 10676–10689.
27. Sorensen, B. R., and Shea, M. A. (1998) Interactions between domains of apo calmodulin alter calcium binding and stability. *Biochemistry 37*, 4244–4253.
28. Faga, L. A., Sorensen, B. R., VanScyoc, W. S., and Shea, M. A. (2003) Basic interdomain boundary residues in calmodulin decrease calcium affinity of sites I and II by stabilizing helix-helix interactions. *Proteins 50*, 381–391.
29. Sorensen, B. R., Faga, L. A., Hultman, R., and Shea, M. A. (2002) An interdomain linker increases the thermostability and decreases the calcium affinity of the calmodulin N-domain. *Biochemistry 41*, 15–20.
30. Chen, B., Mayer, M. U., Markillie, L. M., Stenoien, D. L., and Squier, T. C. (2005) Dynamic motion of helix A in the amino-terminal domain of calmodulin is stabilized upon calcium activation. *Biochemistry 44*, 905–914.
31. Chen, B., Mayer, M. U., and Squier, T. C. (2005) Structural uncoupling between opposing domains of oxidized calmodulin underlies the enhanced binding affinity and inhibition of the plasma membrane Ca-ATPase. *Biochemistry 44*, 4737–4747.
32. Montejano, H., Gervaldo, M., and Bertolotti, S. (2005) The excited-states quenching of resazurin and resorufin by p-benzoquinones in polar solvents. *Dyes Pigments 64*, 117–124.
33. Chen, B., Cao, H., Yan, P., Mayer, M. U., and Squier, T. C. (2007) Identification of an orthogonal peptide binding motif for biarsenical multiuse affinity probes. *Bioconjugate Chem. 18*, 1259–1265.
34. Adams, S. R., Campbell, R. E., Gross, L. A., Martin, B. R., Walkup, G. K., Yao, Y., Llopis, J., and Tsien, R. Y. (2002) New biarsenical ligands and tetracysteine motifs for protein labeling in vitro and in vivo: synthesis and biological applications. *J. Am. Chem. Soc. 124*, 6063–6076.
35. Luedtke, N. W., Dexter, R. J., Fried, D. B., and Schepartz, A. (2007) Surveying polypeptide and protein domain conformation and association with FlAsH and ReAsH. *Nat. Chem. Biol. 3*, 779–784.
36. Martin, B. R., Giepmans, B. N., Adams, S. R., and Tsien, R. Y. (2005) Mammalian cell-based optimization of the biarsenical-binding tetracysteine motif for improved fluorescence and affinity. *Nat. Biotechnol. 23*, 1308–1314.
37. Bartlett, R. K., Bieber Urbauer, R. J., Anbanandam, A., Smallwood, H. S., Urbauer, J. L., and Squier, T. C. (2003) Oxidation of Met144 and Met145 in calmodulin blocks calmodulin dependent activation of the plasma membrane Ca-ATPase. *Biochemistry 42*, 3231–3238.
38. Anbanandam, A., Bieber Urbauer, R. J., Bartlett, R. K., Smallwood, H. S., Squier, T. C., and Urbauer, J. L. (2005) Mediating molecular recognition by methionine oxidation: conformational switching by oxidation of methionine in the carboxyl-terminal domain of calmodulin. *Biochemistry 44*, 9486–9496.
39. Urbauer, J. L., Short, J. H., Dow, L. K., and Wand, A. J. (1995) Structural analysis of a novel interaction by calmodulin: high-affinity binding of a peptide in the absence of calcium. *Biochemistry 34*, 8099–8109.
40. Klee, C. B., Crouch, T. H., and Krinks, M. H. (1979) Calcineurin: a calcium- and calmodulin-binding protein of the nervous system. *Proc. Natl. Acad. Sci. U.S.A. 76*, 6270–6273.
41. Strasburg, G. M., Hogan, M., Birmachu, W., Thomas, D. D., and Louis, C. F. (1988) Site-specific derivatives of wheat germ calmodulin. Interactions with troponin and sarcoplasmic reticulum. *J. Biol. Chem. 263*, 542–548.
42. Matthews, J. C. (1993) *Fundamentals of Receptor, Enzyme, and Transport Kinetics*, pp 50−54, CRC Press, Boca Raton, FL.
43. Griffin, B. A., Adams, S. R., and Tsien, R. Y. (1998) Specific covalent labeling of recombinant protein molecules inside live cells. *Science 281*, 269–272.
44. VanScyoc, W. S., and Shea, M. A. (2001) Phenylalanine fluorescence studies of calcium binding to N-domain fragments of Paramecium calmodulin mutants show increased calcium affinity correlates with increased disorder. *Protein Sci. 10*, 1758–1768.
45. Kilhoffer, M. C., Kubina, M., Travers, F., and Haiech, J. (1992) Use of engineered proteins with internal tryptophan reporter groups and pertubation techniques to probe the mechanism of ligand-protein interactions: investigation of the mechanism of calcium binding to calmodulin. *Biochemistry 31*, 8098–8106.
46. Klevit, R. E., Dalgarno, D. C., Levine, B. A., and Williams, R. J. (1984) ^{1}H-NMR studies of calmodulin. The nature of the Ca^{2+}-dependent conformational change. *Eur. J. Biochem. 139*, 109–114.
47. Chou, J. J., Li, S., Klee, C. B., and Bax, A. (2001) Solution structure of Ca(2+)-calmodulin reveals flexible hand-like properties of its domains. *Nat. Struct. Biol. 8*, 990–997.
48. Goto, K., Toyama, A., Takeuchi, H., Takayama, K., Saito, T., Iwamoto, M., Yeh, J. Z., and Narahashi, T. (2004) Ca^{2+} binding sites in calmodulin and troponin C alter interhelical angle movements. *FEBS Lett. 561*, 51–57.
49. LaPorte, D. C., Wierman, B. M., and Storm, D. R. (1980) Calcium-induced exposure of a hydrophobic surface on calmodulin. *Biochemistry 19*, 3814–3819.
50. Yang, C., Jas, G. S., and Kuczera, K. (2004) Structure, dynamics and interaction with kinase targets: computer simulations of calmodulin. *Biochim. Biophys. Acta 1697*, 289–300.
51. Creighton, T. (1993) *Proteins: Structures and Molecular Properties*, 2nd ed., W. H. Freeman and Co., New York.
52. Small, E. W., and Anderson, S. R. (1988) Fluorescence anisotropy decay demonstrates calcium-dependent shape changes in photo-cross-linked calmodulin. *Biochemistry 27*, 419–428.
53. Jaren, O. R., Kranz, J. K., Sorensen, B. R., Wand, A. J., and Shea, M. A. (2002) Calcium-induced conformational switching of Paramecium calmodulin provides evidence for domain coupling. *Biochemistry 41*, 14158–14166.
54. VanScyoc, W. S., Sorensen, B. R., Rusinova, E., Laws, W. R., Ross, J. B., and Shea, M. A. (2002) Calcium binding to calmodulin mutants monitored by domain-specific intrinsic phenylalanine and tyrosine fluorescence. *Biophys. J. 83*, 2767–2780.
55. Kuboniwa, H., Tjandra, N., Grzesiek, S., Ren, H., Klee, C. B., and Bax, A. (1995) Solution structure of calcium-free calmodulin. *Nat. Struct. Biol. 2*, 768–776.
56. Wilson, M. A., and Brunger, A. T. (2000) The 1.0 Å crystal structure of Ca(2+)-bound calmodulin: an analysis of disorder and implications for functionally relevant plasticity. *J. Mol. Biol. 301*, 1237–1256.
57. Bigelow, D. J., and Squier, T. C. (2005) Redox modulation of cellular signaling and metabolism through reversible oxidation of methionine sensors in calcium regulatory proteins. *Biochim. Biophys. Acta 1703*, 121–134.
58. Gao, J., Yao, Y., and Squier, T. C. (2001) Oxidatively modified calmodulin binds to the plasma membrane Ca-ATPase in a nonproductive and conformationally disordered complex. *Biophys. J. 80*, 1791–1801.
59. Yao, Y., Yin, D., Jas, G. S., Kuczer, K., Williams, T. D., Schoneich, C., and Squier, T. C. (1996) Oxidative modification of a carboxyl-terminal vicinal methionine in calmodulin by hydrogen peroxide inhibits calmodulin-dependent activation of the plasma membrane Ca-ATPase. *Biochemistry 35*, 2767–2787.
60. Yin, D., Kuczera, K., and Squier, T. C. (2000) The sensitivity of carboxyl-terminal methionines in calmodulin isoforms to oxidation by H_2O_2 modulates the ability to activate the plasma membrane Ca-ATPase. *Chem. Res. Toxicol. 13*, 103–110.
61. Boschek, C. B., Jones, T. E., Smallwood, H. S., Squier, T. C., and Bigelow, D. J. (2008) Loss of the calmodulin-dependent inhibition of the RyR1 calcium release channel upon oxidation of methionines in calmodulin. *Biochemistry 47*, 131–142.
62. Gao, J., Yin, D., Yao, Y., Williams, T. D., and Squier, T. C. (1998) Progressive decline in the ability of calmodulin isolated from aged brain to activate the plasma membrane Ca-ATPase. *Biochemistry 37*, 9536–9548.
63. Montgomery, H. J., Bartlett, R., Perdicakis, B., Jervis, E., Squier, T. C., and Guillemette, J. G. (2003) Activation of constitutive nitric oxide synthases by oxidized calmodulin mutants. *Biochemistry 42*, 7759–7768.
64. Smallwood, H. S., Lourette, N. M., Boschek, C. B., Bigelow, D. J., Smith, R. D., Pasa-Tolic, L., and Squier, T. C. (2007) Identification of a denitrase activity against calmodulin in activated macrophages using high-field liquid chromatography-FTICR mass spectrometry. *Biochemistry 46*, 10498–10505.
65. Lafitte, D., Tsvetkov, P. O., Devred, F., Toci, R., Barras, F., Briand, C., Makarov, A. A., and Haiech, J. (2002) Cation binding mode of fully oxidised calmodulin explained by the unfolding of the apostate. *Biochim. Biophys. Acta 1600*, 105–110.
66. Mukherjea, P., Maune, J. F., and Beckingham, K. (1996) Interlobe communication in multiple calcium-binding site mutants of Drosophila calmodulin. *Protein Sci. 5*, 468–477.
67. Sayle, R. A., and Milner-White, E. J. (1995) RASMOL: biomolecular graphics for all. *Trends Biochem. Sci. 20*, 374.

BI800566U